Supporting Information

for

Electroosmotically Driven Microfluidic Actuators

Menake E. Piyasena, Robert Newby, Thomas J. Miller, Benjamin Shapiro, and Elisabeth Smela

The theoretical calculations for device performance are shown in detail in sections 1-6. In section 7 the experimental work done by the actuator is plotted as a function of applied force. In section 8 we present simulations of multi-cell deformations.

1 Variables

Table I. Variable values.

	Symbol	Values	Units	SI Value	SI Units
Device Dimensions					
<u>membrane-covered reservoirs</u>					
reservoir length	l_r	5.0	mm	5.00E-03	m
reservoir width	w_r	2.5	mm	2.50E-03	m
PDMS membrane thickness	h	25	μm	2.50E-05	m
round membrane equivalent radius	r	1.995	mm	1.995E-03	m
<u>channels</u>					
number of channels	n	9		9	
channel depth	d_c	25	μm	6.00E-05	m
channel width	w_c	150	μm	1.50E-04	m
channel length	l_c	1	cm	1.00E-02	m
<u>electrodes</u>					
distance between electrodes	L	3	cm	3.00E-02	m
Actuation					
applied voltage	V	3.5	kV	3,500	V
time required to inflate membrane	t_i	5	sec	5	sec
membrane deflection	h	120	μm	1.20E-04	m
time required to deflate membrane	t_d	2	sec	2	sec

Material Constants/Properties

dielectric constant of fluid	ε	78		78	
zeta potential	ζ	0. 05	V	2.00E-02	V
viscosity of the liquid	η	0.001	$N{\cdot}s/m^2$	1.00E-03	Pa·s
membrane Young's modulus	E_Y	0.5	MPa	5.00E+05	Pa
membrane Poisson's ratio	ν	0.4		4.00E-01	
Constants					
permittivity	ε_0	8.9E-12	C^2/Nm^2	8.9E-12	C/Vm
gravitational constant	g			9.8	m/s^2

2 Flow Rate Due to EOF

2.1 Experimental EOF Flow Rate

To calculate the experimental flow rate, the volume of fluid in the membrane above the reservoir is divided by the time required to inflate the membrane. The volume *V* can be approximated as half the volume of a scalene ellipsoid

(1) $$V = \frac{1}{2}\left(\frac{4}{3}\pi abc\right)$$

where *a* is half the length of the major axis ($l_r/2$), *b* is half the length of the minor axis ($w_r/2$), and *c* is the deflected height of the membrane. To obtain the flow rate over most of the inflation period, take the values to reach 80% of the final height of 120 μm (Figure 3D in the main text.) Using the values in Table I, for a deflection of 120 μm * 0.80 = 96 μm,

(2) $V = 0.63$ μL.

It takes 5 seconds to reach that height under an applied voltage of 3.5 kV, giving a flow rate of

(3) $Q_{EO} = dV/dt = 0.126$ μL/sec.

To check this answer, one can also approximate the volume as the section of a hemisphere above the surface of the reservoir. The radius *R* of the circle, of which the expanded region is an arc, changes as the membrane inflates. It is related to the inflated height *h* and the diameter *L* as follows.

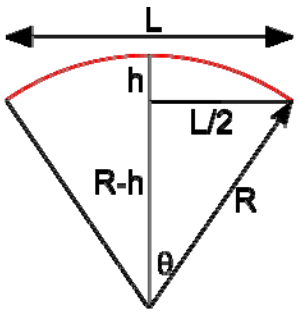

(4)
$$R^2 = (R-h)^2 + L^2/4$$
$$R^2 = R^2 - 2Rh + h^2 + L^2/4$$
$$2Rh = h^2 + L^2/4$$
$$R = \frac{h^2 + L^2/4}{2h} = \frac{4h^2 + L^2}{8h}$$

To calculate the volume of the expanded area, integrate the area over the distance above the surface.

(5)
$$V = \int_y^R \pi(R^2 - x^2)dx = \pi(R^2 x - x^3/3)\Big|_y^R$$
$$= \pi(R^3 - R^2 y - R^3/3 + y^3/3) = \pi(\frac{2}{3}R^3 - R^2 y + y^3/3)$$

Setting y = R – h and doing the algebra, we obtain

(6)
$$V = \frac{\pi}{3}(3Rh^2 - h^3).$$

Using an equivalent diameter of

(7)
$$r = \sqrt{ab/\pi}$$

and again using h = 96 μm gives V = 0.60 μL. This is nearly the same as the volume as found above.

2.2 Theoretical EOF Flow Rate

The flow due to EOF is found by defining an electroosmotic mobility μ_{EO} [1]

(8)
$$\mu_{EO} = \frac{\varepsilon\varepsilon_0\zeta}{\eta}$$

where ε is the dielectric constant, ε_0 is the permittivity, ζ is the zeta potential, and η is the fluid viscosity. The zeta potential depends on the chemistry of the fluid/channel wall system. Applying an electric field $\vec{E}$ produces an electroosmotic velocity v_{EO}

(9)
$$v_{EO} = \mu_{EO}|\vec{E}|$$

To obtain the flow rate, the velocity is multiplied by the cross sectional area A available for flow, which is the number of channels n times their width w_c and depth d_c.

(10) $$Q_{EO} = Av_{EO} = nw_c d_c \frac{\varepsilon\varepsilon_0\zeta}{\eta}|\vec{E}|$$

Using an estimate of $\zeta = 0.05$ V, for an applied voltage of 3.5 kV we obtain

(11) $Q_{EO} = 0.14$ μL/sec.

This is the same as the experimental value.

3 Flow Rate Due to Pressure

3.1 Experimental Pressure-Driven Flow Rate

When EOF is turned off, the elastic restoring forces of the membrane push the fluid back down. The time required to empty the reservoir, from a deflection of 120 μm (see Figure 3D), is two seconds. Calculating the fluid volume in the same manner as above gives $V = 0.785$ μL. This results in a relaxation flow rate Q_P of

(12) $Q_P = V/t = 0.393$ μL/sec.

3.2 Theoretical Pressure-Driven Flow

3.2.1 Pressure Applied by the Membrane

The relationship between the flow rate Q_P and pressure difference ΔP for n rectangular channels due to a pressure gradient across the channels is [2]

(13) $$Q_P = n\frac{d_c^3 w_c}{12\eta l_c}\Delta P\left[1-0.63\frac{d_c}{w_c}\right]$$

where l_c is the length of the channel. Using the experimental relaxation flow rate, we can find the pressure on the membrane. Rearranging,

(14) $$\Delta P = \frac{12\eta l_c}{n d_c^3 w_c}\frac{1}{\left[1-0.63 d_c / w_c\right]}Q_P$$

Using 0.393 μL/sec and the values in Table I, we find a relaxation pressure of

(15) ΔP = 2500 Pa.

3.2.2 Pressure Due to EOF

By equating the flow rates due to EO, equation (10), and the membrane, equation (12), we can obtain the pressure due to EO flow, ΔP_{EO}.

(16) $$\Delta P_{EO} = 12 l_c \varepsilon\varepsilon_0\zeta\left|\vec{E}\right| / d_c^2\left[1-0.63 d_c / w_c\right]$$

Note that this does not depend on the number of channels. Using the values in Table I we obtain

(17) ΔP_{EO} = 870 Pa.

Since it took over 5 seconds to fill and 2 seconds to empty the fluid above the reservoir, we would have expected a pressure of less than approximately 2500 * 2 / 5 = 1000 Pa, which is consistent with the calculated value.

4 Membrane Deflection Due to EOF

The deflection *y* of the center of a rectangular membrane due to a pressure *P* is [3]

(18) $$P = \frac{\pi^6}{64}\left\{4Dy\left(\frac{1}{a^2}+\frac{1}{b^2}\right)^2 + \frac{Ety^3}{4}\left(\frac{1}{a^4}+\frac{1}{b^4}\right) + \frac{Ety^3}{2(1-\nu^2)}\left[\frac{2}{a^2b^2}+\nu\left(\frac{1}{a^4}+\frac{1}{b^4}\right)\right]\right\}$$

where D is the flexural rigidity,

(19) $$\mathrm{D} = Et^3 / \left[12(1-\nu^2)\right],$$

E is the Young's modulus, and ν is the Poisson ratio. A pressure of 870 Pa is expected to produce a deflection of

(20) y = 239 μm.

This is very close to the deflection of 280 μm observed experimentally at 3.5 kV.

The deflection is plotted below as a function of pressure using the relationship in equation (18).

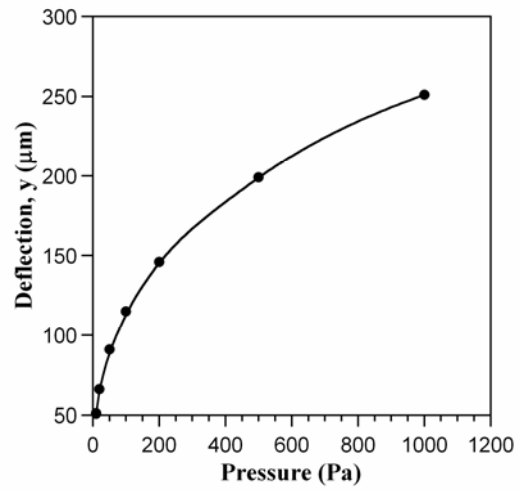

The contribution of each of the three terms in the equation to the total pressure is shown in the following figure. The 2nd and 3rd terms dominate, with the 3rd term being twice as large as the second.

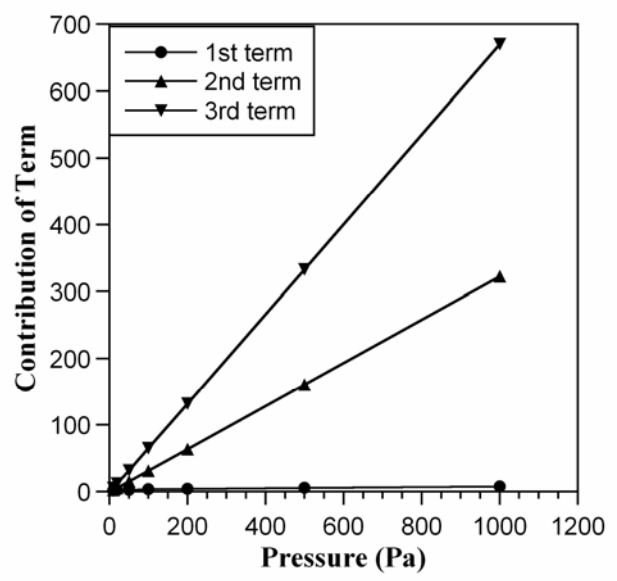

5 Force Due to EOF

The area of the membrane is $A = w_r * l_r = 12.5$ mm^2. The pressure is a force per unit area, so multiplying the pressure by the area should yield the force that can be exerted by the membrane. Experimentally, the blocking force for 3.5 kV was on the order of 1 gram. Using the area of the entire membrane and a pressure of 870 Pa, theoretically we would expect

(21) $F = A * \Delta P_{EO} = 1.25 * 10^{-5}$ m^2 * 870 N/m^2 = $1.1*10^{-2}$ N.

This corresponds to weight of

(22) $1.1*10^{-2}$ N / 9.8 m/sec^2 = 1.1 g

This is close to the experimentally estimated blocked force of 1.2 g at 3.5 kV.

6 Calculating Tensile Strain

Returning to the figure in section 2.1 above, and using L = 2.5 mm, which is the length of the shortest side of the reservoir, we can obtain the length of the arc (the red line) by

(23) $\sin\theta = (L/2)/R$

and

(24) arclength = $2\pi R * 2\theta /360$

The strain is found from $\Delta L/L$ where ΔL = arclength – L. For h = 240 μm, R = 3.4 mm, θ = 21.7°, and the arclength = 2.56 mm, giving ΔL = 0.06 mm and a strain of 2.4%. Beyond h = 1.25, for which strain = 57%, the shape is no longer an arc of a circle.

7 Work

The work performed by the actuator at different applied voltages is shown here.

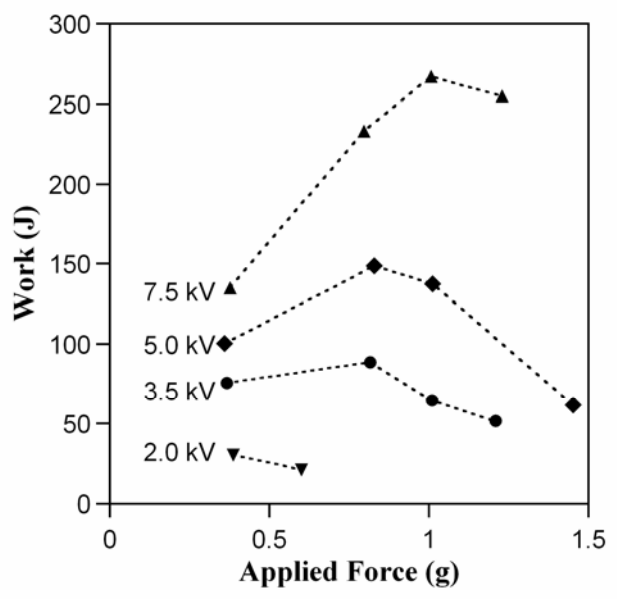

8 Simulations of Multi-Cell Deformations

Simulations of multi-cell material deformations, as shown in Figure 4A, B in the main text, were carried out as follows. For a single cell, the material was treated as linearly elastic. Equation (3) in the main text gave the pressure difference between the supply and expansion chambers. This pressure was applied as a boundary condition to the internal reservoir boundaries, as shown below. The resulting material deformation was assumed to be governed by standard elasticity equations and was computed using the multi-physics COMSOL software (www.comsol.com). COMSOL uses a finite element method and has a moving mesh capability that can keep track of large material deformations. A Lagrangian method was used wherein the mesh followed the motion of the material.

The figure below shows the model setup in two spatial dimensions for a single cell. The boundary conditions are shown in panel a): EO actuation creates a pressure difference in the reservoirs (pressure in on the left, pressure out on the right), the position of the channel is fixed (to prevent rigid body translations/rotations), and the free edges of the material have zero stress. Panel b) shows the mesh deforming with the material elements. Panel c) shows the resulting material deformation, colored by the von Mises stresses.

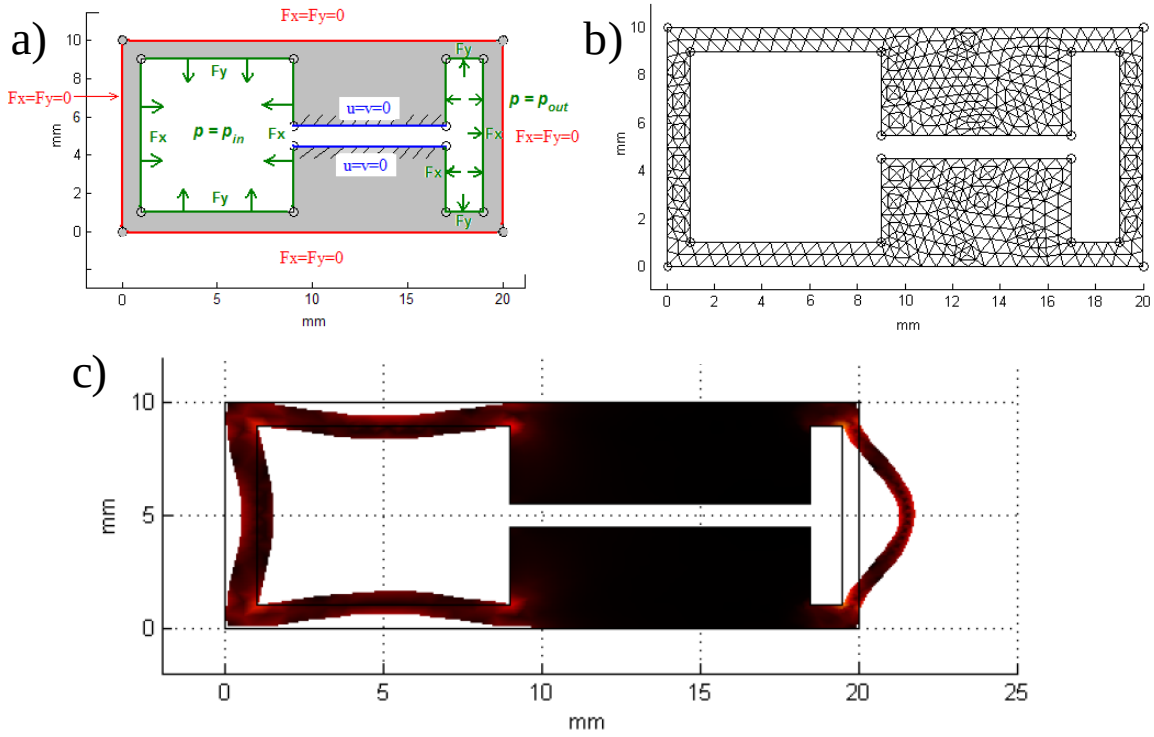

Simulations for a collection of cells, and for 3-dimensions, were done the same way, with the same boundary conditions repeated throughout. In the multi-cell simulations, two edge points were constrained to remain fixed in the y direction, and a center material point was constrained to remain fixed in the x direction; this allowed arbitrary deformation of the material but prevented rigid body translations and rotations.

9 References

[1] J. P. Kutter, K. B. Mogensen, H. Klank, O. Geschke, "Microfluidics -- Components," in *Microsystem Engineering of Lab-on-a-chip Devices* (Eds: O. Geschke, H. Klank, P. Telleman) Wiley-VCH, Weinheim, **2004**, p. 39-77.

[2] H. Bruus, *Theoretical Microfluidics*, Oxford University Press, New York, **2008**, p. 51.

[3] D. Wang, A. I. El-Sheikh, "Large-deflection mathematical analysis of rectangular plates," *J. Eng. Mechanics*, **2005**, *131 (8)*, 809-21.